

ABSTRACT

We introduce a new algorithm for tracking 3D seismic horizons. The algorithm combines an inversion-based, **seismic-dip** flattening technique with conventional, similarity-based auto-tracking. The inversion part of the algorithm aims to minimize the error between horizon dips and computed seismic dips. After each cycle in the inversion loop, more seeds are added to the horizon by the similarity-based auto-tracker. In the example data set, the algorithm is first used to quickly track a set of framework horizons, each guided by a small set of user-picked seed positions. Next, the intervals bounded by the framework horizons are infilled to generate a dense set of horizons, a.k.a. HorizonCube. This is done under supervision of a human interpreter in a similar manner. The results show that the algorithm behaves better than unconstrained flattening techniques in intervals with trackable events. Inversion-based algorithms generate continuous horizons with no holes to be filled **post-tracking** with a gridding algorithm and no loop-skips (**jumping to the wrong event**) that need to be edited as is standard practice with auto-trackers. As **editing** is a time consuming process, creating horizons with inversion-based algorithms tends to be faster than **conventional** auto-tracking. Horizons created with the proposed algorithm follow seismic events more closely than horizons generated with the inversion-only algorithm and fault crossings are sharper.

INTRODUCTION

Since horizon tracking is an essential, difficult and time-consuming part of seismic interpretation, numerous algorithms and workflows have been developed since the introduction of seismic interpretation workstations in the 1980s. The first landmark paper on horizon tracking only considered amplitude values to follow seismic peaks, troughs and zero-crossings (Howard, 1991).

This method works well for fairly continuous reflectors but it breaks down in more difficult conditions such as in the presence of faults and with laterally changing reflectors. A good summary of the early history of horizon tracking is given by Dorn (1998). A significant improvement was the introduction of cross-correlations, which enable tracking across faults (e.g. Aurnhammer and Tönnies, 2005; Admasu and Tönnies, 2004).

The introduction of global seismic interpretation methods revolutionized seismic interpretation workflows in the last decade and increased the amount of geologic information that is nowadays extracted routinely from the data (de Groot et al., 2016). Global seismic interpretation methods can be defined as automated or semi-automated methods that aim to generate fully interpreted volumes (Stark, 2004; Lomask et al., 2006; de Groot et al., 2010; Hoyes and Cheret, 2011; Dirstein and Fallon, 2012; Labrunye and Jayr, 2013; Stark et al., 2013). The fully interpreted volumes created by these methods increase our understanding of depositional histories and are instrumental to finding stratigraphic traps, and these algorithms enable the construction of more accurate geological models in less time.

Global methods differ in the way they correlate seismic events, in how they store results (in a regularly sampled volume, or as a dense set of horizons), and in the way - and amount of user interaction. Based on technology, global methods can be grouped into three categories:

1. Event Correlation
2. Artificial Intelligence (AI)
3. Flattening.

Each method has its pros and cons. Methods based on event correlation evolved from conventional amplitude and similarity trackers. The modern variant is inversion-based (Pauget et al., 2009). It outputs a 3D grid model by connecting each seismic event (min, max and zero-crossings) to the

most probable neighboring events. Event correlation-based methods are robust but also prone to loop-skips (**jumps to erroneous events**) which require human intervention. Furthermore, event-based techniques struggle with correlating laterally varying events such as unconformities, which are key events in seismic sequence stratigraphic analysis.

Methods based on AI, especially those using deep learning algorithms, show potential (Grimsgaard, 2019; Gupta et al, 2019) but more research and development is needed before these methods reach the market and can be applied in operational settings. **AI methods need large amounts of (accurate) training data, which is difficult to generate. Furthermore, training deep learning algorithms is a time-consuming process. Finally, results need checking and editing manually by the user, which is also time-consuming.** A global seismic interpretation method based on AI is already on the market. Dirstein and Fallon (2012) use genetic algorithms to output horizon patches that are locally accurate but the patchy nature of the output limits its usefulness. Bugge et al. (2018) present a combination of supervised - and unsupervised learning methods and dynamic time warping (Hale 2013) to produce horizon patches in regions with extensive faults. Their workflow is fully automated but the results also require checking and editing.

Flattening methods are inversion-based techniques that aim to flatten the seismic dip field (Lomask et al., 2006; de Groot et al., 2010; Wu and Hale, 2013). As these methods do not operate on seismic amplitudes but instead use the dip field as input they are capable of mapping unconformities. A disadvantage of flattening is that the resulting horizons are not necessarily phase-consistent. In other words, horizons may drift around seismic events instead of following these exactly. **To overcome this problem Wu and Fomel (2018) combine local reflection slopes (Yu et al., 2012; Hale, 2009) and multi-grid correlations obtained by dynamic time warping (Hale, 2013). The horizons shown in Wu and Fomel's paper indeed seem to be phase-consistent but we were not able to achieve the desired level of phase-consistency in our own experiments with this algorithm. We**

therefore decided to develop an alternative method, which is presented hereafter as the hybrid algorithm.

Horizons generated with inversion-based flattening algorithms are continuous, i.e. they exist at every seismic position where dip information exists. Conventional auto-trackers usually require filling holes and editing loop-skips. Filling holes with a gridding algorithm is inaccurate and editing is time-consuming and laborious. The workflow for inversion-based flattening is faster. The interpreter QC's (Quality Control's) horizons, adds seeds where needed, and re-runs the inversion until satisfied. The inversion itself is fast and parallelized. To create 4 horizons in the Delft survey (84 km²) took 40 seconds on a Windows 10 machine with four 2.5 GHz Cores and 32GB RAM.

The algorithm discussed in this paper is a hybrid method that combines inversion-based flattening with event correlation. We will compare the proposed hybrid algorithm with the underlying algorithms: inversion-based flattening and similarity-based auto-tracking. We will show that the hybrid method improves phase-consistency in intervals with correlatable events. Furthermore, we will argue and demonstrate that both inversion-based algorithms are needed in the creation of a dense set of horizons for the example data set.

METHODOLOGY

The inversion-based flattening part of the hybrid algorithm is an implementation of the algorithm proposed by Wu and Hale (2015). An initial horizon grid is constructed through one or more seed positions, after which an inversion algorithm minimizes the error between horizon dips and seismic dips (Figure 1a). This is done with a constrained conjugate gradient solver. After each iteration loop of the solver the horizon grid is re-tied to the input seeds (Figure 2 - grey blocks). Seismic

dips are pre-computed with a Principal Component Analysis (PCA) based algorithm that outputs local dips in the inline and crossline directions. Prior to inversion-based flattening the dip-field is usually smoothed and denoised with a median filter. Optionally, the PCA-based dip computation algorithm outputs a third component called “planarity” (Wu and Hale, 2013). Planarity is a measurement of the local curvedness of the dip field normalized between 0 and 1. High planarity corresponds to good reflections. Low planarity occurs near faults and in noisy sections. Planarity is used by the inversion algorithm to assign higher weights to areas with good reflections.

The similarity-based auto-tracker in this paper starts from one or more manually picked seed positions that are snapped to a seismic event. The tracker compares (relative) amplitude differences and cross-correlations between seed traces and traces located at the edges of the growing horizon grid. Positions are added to the grid if the acceptance criteria are met. This tracking mode is used in the exercise in which we compare the three algorithms (next section). In the hybrid algorithm, the decision to add seed positions is based not on relative amplitude differences but only on cross-correlation thresholds.

Recommended position for Figure 1

In the hybrid tracker, the two algorithms are combined (Figure 2 - grey + yellow blocks). Again the horizon is constrained with one or more manually picked seeds. In contrast to the inversion-based flattening on dip only, the hybrid algorithm snaps seed positions to the nearest event, i.e. either to a maximum or a minimum. An initial horizon grid is constructed through the seed positions and the conjugate gradient solver is started. After each inversion cycle, the similarity auto-tracker kicks in to add additional (snapped) seed positions (Figure 2). The horizon grid is tied to the new seeds and the process continues until the end-criteria of the inversion loop are met.

Recommended position for Figure 2

NETHERLANDS DATA SET

The data set is a time-converted subset of a 3D Prestack Depth Migration (PSDM) volume covering the city of Delft. The data was acquired in 1985 by NAM and re-processed in 2011. The bin-size is 20 m by 20 m and the temporal sampling rate is 4 ms. The data is zero-phase, non-SEG polarity meaning a hard-kick is a negative number. The areal coverage of the subset is 84 km².

Oil and gas have been produced in this area since the 1950's but most onshore fields were abandoned around 1994. Oil was produced from early Cretaceous sands while gas was produced from Germanic Triassic sandstones of the Bundsandstein sub-group. With the Netherlands' drive towards renewable energy, the interest in exploring for oil and gas has now shifted towards geothermal energy. In the study area, two geothermal systems have been operational since 2010 and a third installation is being planned.

RESULTS

Figure 3 shows three horizons created with the hybrid algorithm. The upper horizon (pink) is the Base Upper North Sea, an important break in sedimentation around the Oligocene-Miocene boundary. The group consists of shallow-marine sediments, mainly deposited in the western Netherlands, and of terrestrial beds of fluvial, paralic, and lacustrine origin. In the upper part glacial deposits occur (DINO, 2019). The boundary corresponds to a hard kick and is displayed as a white loop. The event was tracked through the entire survey from one seed only. The middle horizon (orange) is a hard kick in the Holland Formation, consisting of marine deposits of marls, clays, and sandstones. The mapped Intra-Holland event shows up as a clear white loop that was tracked from two seed positions. The deepest event is also picked on a white loop but this event is more difficult to track. The lateral continuity varies and the interpretation had to be forced through

the faulted zones under the popup structures where seismic quality is poor. To track this horizon required several iterations and dozens of seeds. Even so, the **workflow** was considered to be easier and faster than tracking with a conventional auto-tracker with inherent editing - and post-interpretation infill gridding problems.

Recommended position for Figure 3

Figure 4 shows a comparison of the three algorithms on the deep event depicted in Figure 3. All algorithms used the same set of input seeds. The inversion-based algorithms used the same inputs (seismic dips plus planarity) and input parameters for the conjugate gradient solver. The similarity-based tracker tracked on the basis of relative amplitude differences and cross-correlation thresholds. The parameters were optimized to track as far as possible without creating loop-skips. Nevertheless, as can be seen in Figure 4, the tracker did create some loop-skips and left holes to be filled. The problem of loop-skips can be reduced, albeit at the expense of creating larger holes. If we compare the two inversion-based algorithms with each other we observe that the hybrid tracker better follows the white loop than the tracker that is based only on flattening the dip field.

Recommended position for Figure 4

The dense set of horizons was created **by the user** in three consecutive interpretation steps. First, the user created a set of framework horizons that divided the interval of interest into a manageable set of sequences. Framework horizons can be imported, or they are tracked by one of the algorithms described in this paper. **Since framework horizons represent relative geological timelines** the only criteria imposed on them are: 1) they must be continuous (**meaning they have a Z value at every grid position**), and 2) they cannot cross each other. Figure 5b shows six framework horizons that split the interval above Top Vlieland (**Framework Horizon 6**) into 5 sequences. The Base Tertiary event (**Framework Horizon 3**) is a pronounced unconformity with laterally varying reflection patterns. This event was tracked with the inversion-based flattening algorithm (**dip-only**). The top

horizon is a dummy horizon at $Z = 0$ ms. The four other framework horizons are trackable events that were mapped with the hybrid algorithm.

Recommended position for Figure 5

The next step in the workflow is infill tracking under human supervision. This is done per sequence bounded by framework horizons. The workflow is similar to the one described above: the inversion-based algorithm is run (either dip-only, or hybrid), the results are QC-ed and additional seeds are added. This is repeated until the user is satisfied with the infill horizons in the sequence after which the process is repeated for all sequences. The algorithm ensures that all horizons are continuous and that none of the infill horizons crosses the framework horizons, or each other (Figure 5c).

In the 3rd and final step, more horizons are added to the set to arrive at the desired density for follow-up work including but not limited to: Wheeler transformation (seismic flattening), model building, and seismic sequence stratigraphic interpretation. Infilling at the finest level can be done with the same methods applied in the previous step but in this case it was done with a model-driven algorithm that inserted horizons proportionally between upper and lower bounding horizons (Figure 5d). All horizons, whether created by inversion-based methods, or by model-driven infill, in the set are continuous and no horizon crosses any other horizon in the set. Because of these properties, each horizon in the set can be considered a relative geologic timeline. In other words: a horizon located above another horizon in the same set is per definition younger than a horizon located below. The accuracy of the set is fully user-controlled. First the user controls the accuracy of the framework horizons by re-running the inversion-based algorithms until satisfied. Secondly, the user controls the amount - and accuracy of infilled horizons. More accuracy is obtained by adding more inversion-based infill horizons and re-running the algorithm until satisfied.

CONCLUSIONS

We introduced a hybrid algorithm that can be used to: 1) quickly generate a set of seismic horizons and 2) to create a dense set of horizons. The hybrid algorithm performs better on trackable events than an inversion-based flattening algorithm that only operates on the dip field. The latter is better at tracking laterally varying events such as unconformities (de Groot et al., 2016). Both inversion-based algorithms tend to generate seismic horizons faster than similarity-based auto-trackers. This is because inversion-based algorithms produce continuous horizons that do not require time-consuming loop-skip editing and inaccurate infill gridding. Instead, the interpreter iterates a workflow of three steps: adding seeds, running the inversion, and QC-ing results, until satisfied.

ACKNOWLEDGMENT

We thank Hydreco Geomec BV for permission to use the Netherlands dataset for this publication. We also thank A.J. Bugge and two anonymous reviewers for their constructive criticisms that have led to a better paper.

REFERENCES

Admasu, F., & Tönnies, K. D., 2004, Model-based Approach to Automatic 3D Seismic Horizon Correlation across Faults: SimVis pp. 239-250.

- Aurnhammer, M., & Tonnie, K. D., 2005, A genetic algorithm for automated horizon correlation across faults in seismic images: IEEE Transactions on Evolutionary Computation, v9(2), 201–210.
- Bugge, Aina J., J. E. Lie, and S. Clark, 2018, Automatic facies classification and horizon tracking in 3D seismic data: First EAGE/PESGB Workshop Machine Learning, European Association of Geoscientists & Engineers.
- De Groot, P., Huck, A., De Bruin, G., Hemstra, N., and Bedford, J., 2010, The horizon cube: A step change in seismic interpretation!: The Leading Edge 29, 1048-1055.
- De Groot, P.F.M., Qayyum, F., Liu, Y., and Hemstra, N., 2016, New methods for slicing and dicing seismic volumes: First Break volume 34.
- DINO database, 2019, accessed 30 October 2019, <https://www.dinoloket.nl/en>
- Dirstein, K. and Fallon Gary, J.N., 2012, Automated Interpretation of 3D seismic data using genetic algorithms: ASEG Extended Abstracts 2012, 1-1.
- Dorn, Geoffrey A., 1998, Modern 3-D seismic interpretation: The Leading Edge v17.9, 1262-1262.
- Grimsgaard, J., 2019, Deep Learning Neural Network Solution Applied to Seismic Interpretation: FORCE Hackathon and/or the symposium: Applied Machine Learning and Advanced Analytics with Oil and Gas Data, Stavanger.
- Gupta, H., Pradhan, S., Gogia, R., Srirangarajan, S., Phirani, J., & Ranu, S., 2019, Deep Learning-Based Automatic Horizon Identification from Seismic Data: SPE Annual Technical Conference and Exhibition.
- Hale, D., 2009, Structure-oriented smoothing and semblance: CWP report 635.635.

Hale, D., 2013, Dynamic warping of seismic images: *GEOPHYSICS*, Vol. 78, pp. S105–S115

Hoyes, J., & Cheret, T., 2011, A review of “global” interpretation methods for automated 3D horizon picking: *Leading Edge*, 30(1), 38–47.

Howard, Robert E. , 1991, Method for attribute tracking in seismic data: U.S. Patent No. 5,056,066. 8 Oct. 1991.

Labrunye, E., & Jayr, S., 2013, Merging chronostratigraphic modeling and global interpretation: *SEG Technical Program Expanded Abstracts*, pp. 1430-1434.

Lomask, J., Guitton, A., Fomel, S., Claerbout, J., & Valenciano, A. A., 2006, Flattening without picking: *Geophysics*, 71(4), P13–P20.

Pauget, F., Lacaze, S., & Valding, T., 2009, A global interpretation based on cost function minimization: 79th Annual International Meeting SEG, *Expanded Abstracts*, 2592–2596.

Stark, T., 2004, Relative geologic time (age) volumes—Relating every seismic sample to a geologically reasonable horizon: *The Leading Edge* v23 Issue 8 928-932

Stark, T. J., Zeng, H., & Jackson, A., 2013. An introduction to this special section: *Chronostratigraphy: The Leading Edge*, 32(2), 132-138.

Wu, X., & Hale, D., 2013, Extracting horizons and sequence boundaries from 3D seismic images: *SEG Technical Program Expanded Abstracts 2013*.

Wu, X., and Hale, D., 2015, Horizon Volume with Interpreted Constraints: *Geophysics*, v80, Issue 2, IM21-IM33.

Wu, Xinming, and Sergey Fomel, 2018, Least-squares horizons with local slopes and multigrid correlations: *Geophysics* v83 Issue 4: IM29-IM40.

Yu, Yingwei, Clifford Lee Kelley, and Irina M. Mardanova, 2012, Seismic horizon autopicking using orientation vector field: U.S. Patent No. 8,265,876.

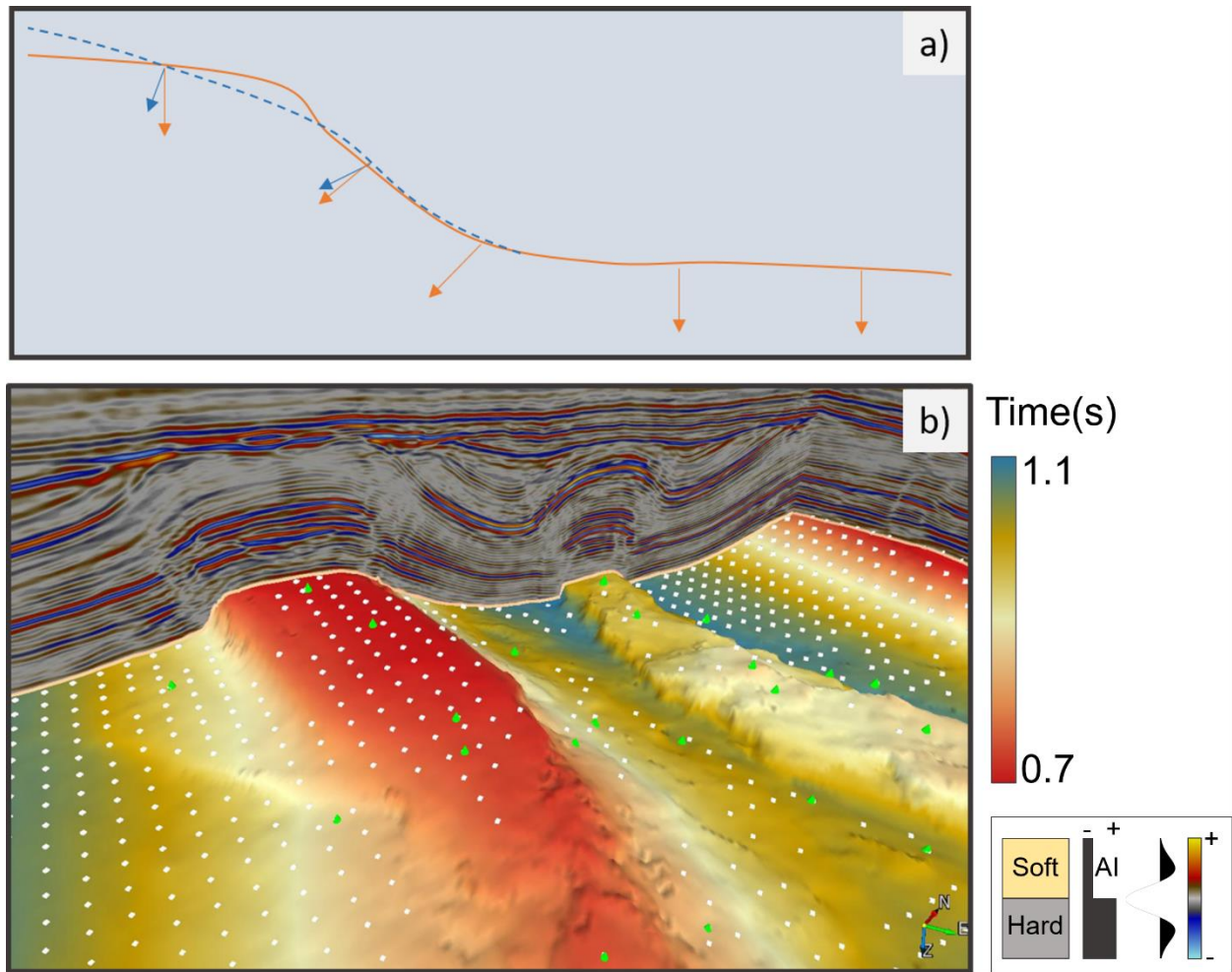


Figure 1. Principle of the hybrid tracker: 1a) An inversion algorithm minimizes the error between horizon grid dips (blue) and pre-computed seismic dips (orange); 1b) The horizon grid is tied to manually picked seed positions (green dots) and auto-generated seeds added by the similarity-based auto-tracker after each inversion cycle (white dots).

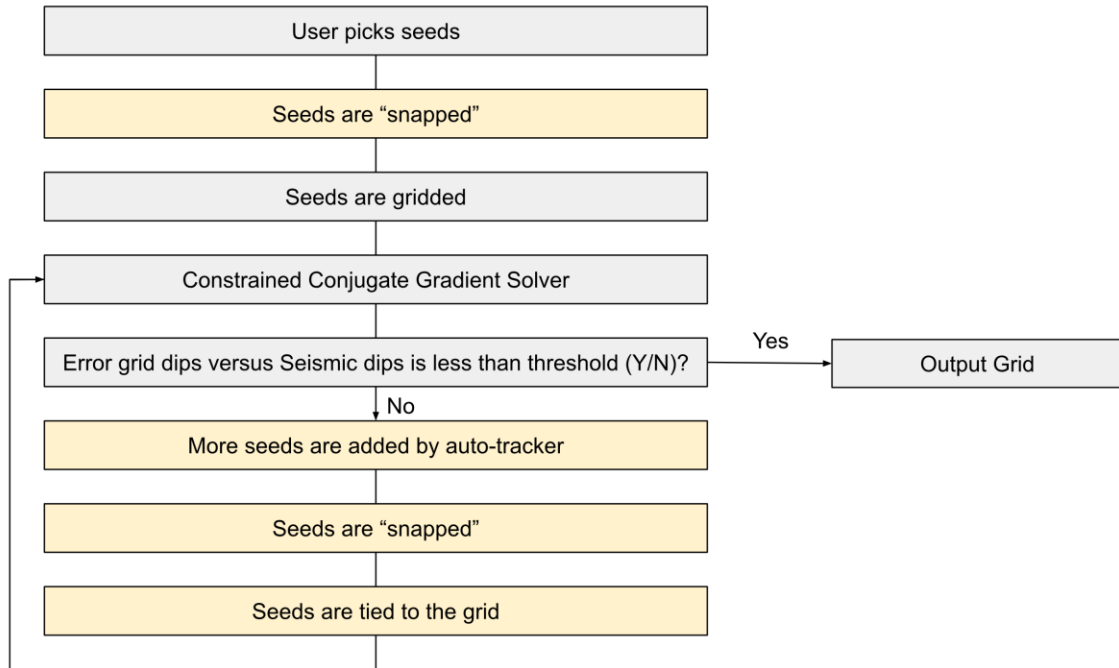


Figure 2. Flowchart of the two inversion-based algorithms described in this paper. The Unconformity Tracker only executes the grey colored steps. The Hybrid Tracker also executes the yellow colored steps.

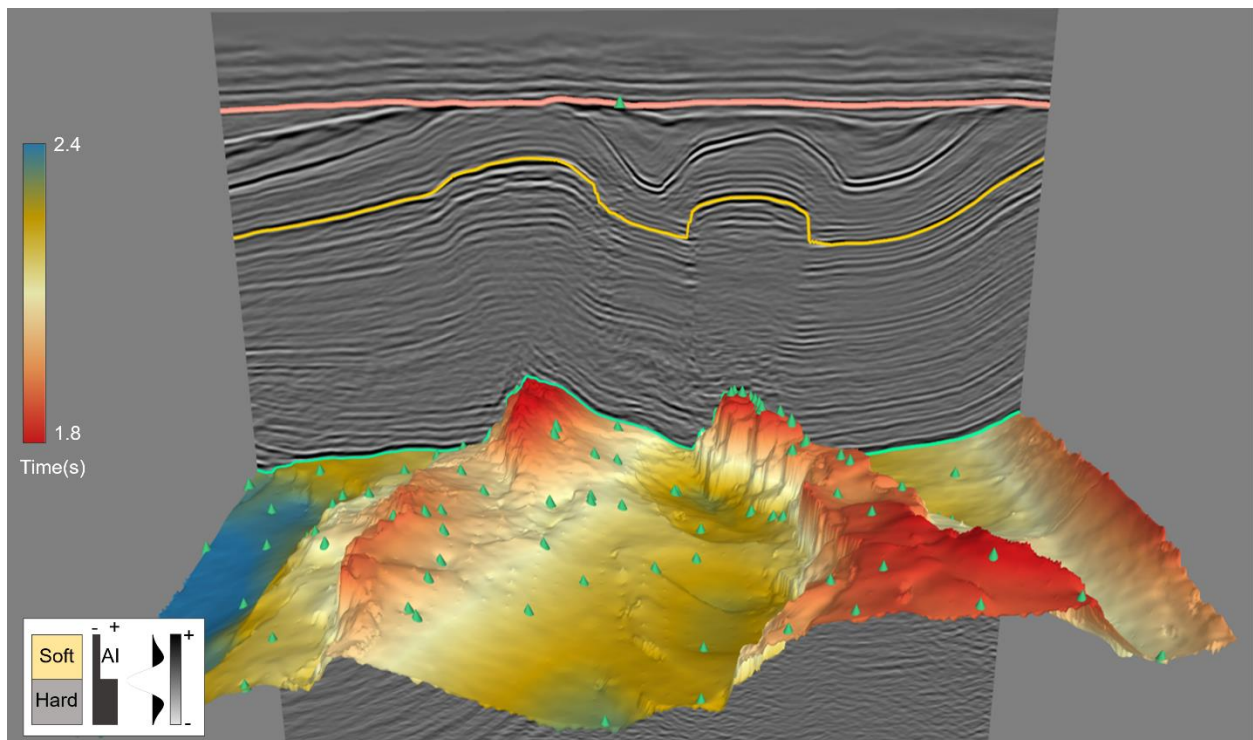


Figure 3. A seismic section with three horizons tracked by the hybrid algorithm. The upper horizon (Base Upper North Sea, salmon color) was tracked from a single seed position. The middle and lower horizons (Intra-Holland (orange) and Deep event (green), respectively) were tracked with multiple seeds and required several QC runs in which seeds were added.

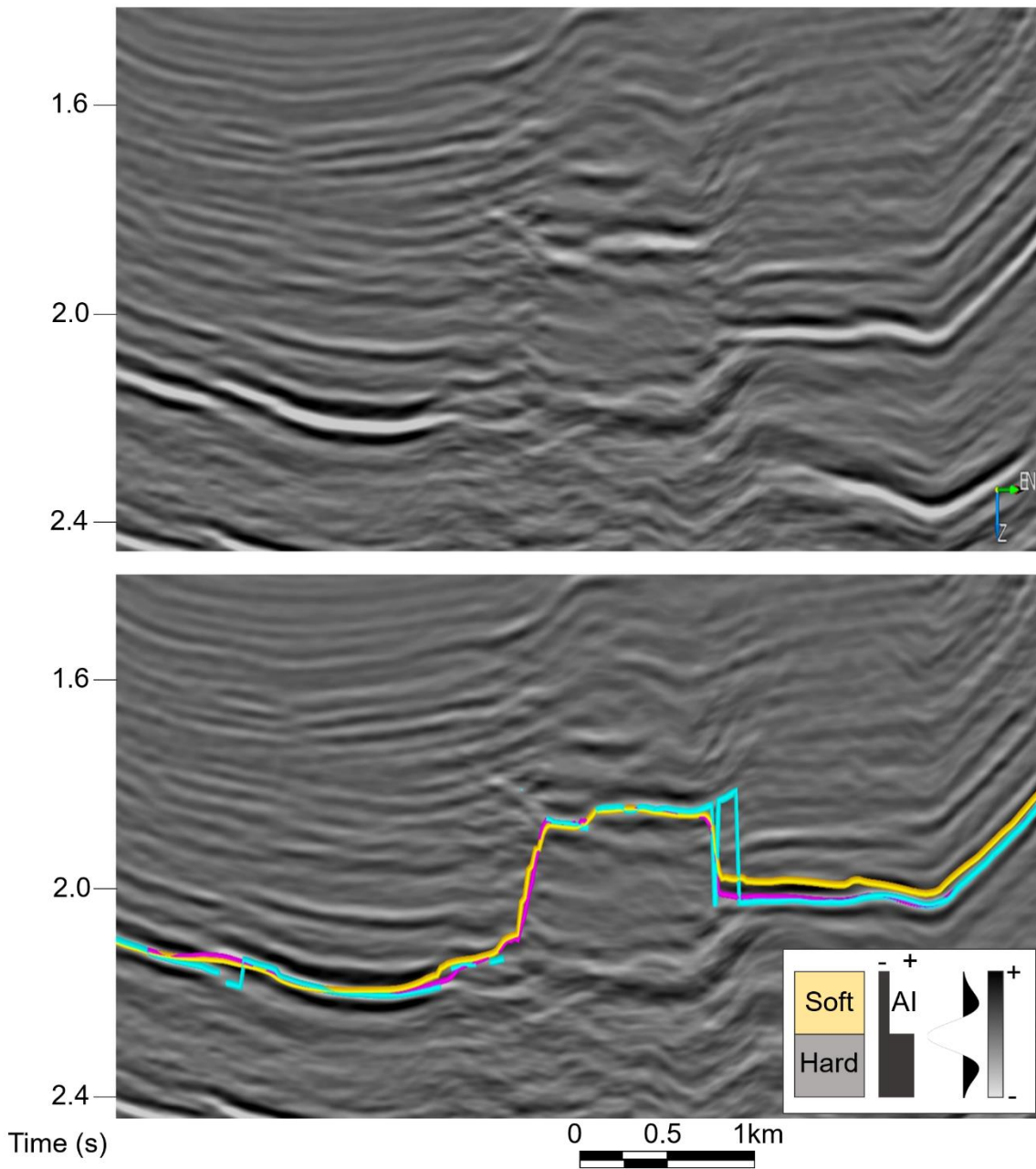


Figure 4. Comparison of tracking algorithms: hybrid algorithm (pink), inversion-based flattening on dip only (yellow), and amplitude & similarity tracking (light blue). Note loopskips and holes in the amplitude & similarity tracked horizon and phase inconsistency of the inversion-based flattening on dip only. The latter is most clearly seen on the right-hand side where the horizon drifts around a black loop instead of staying on the white loop it is supposed to follow.

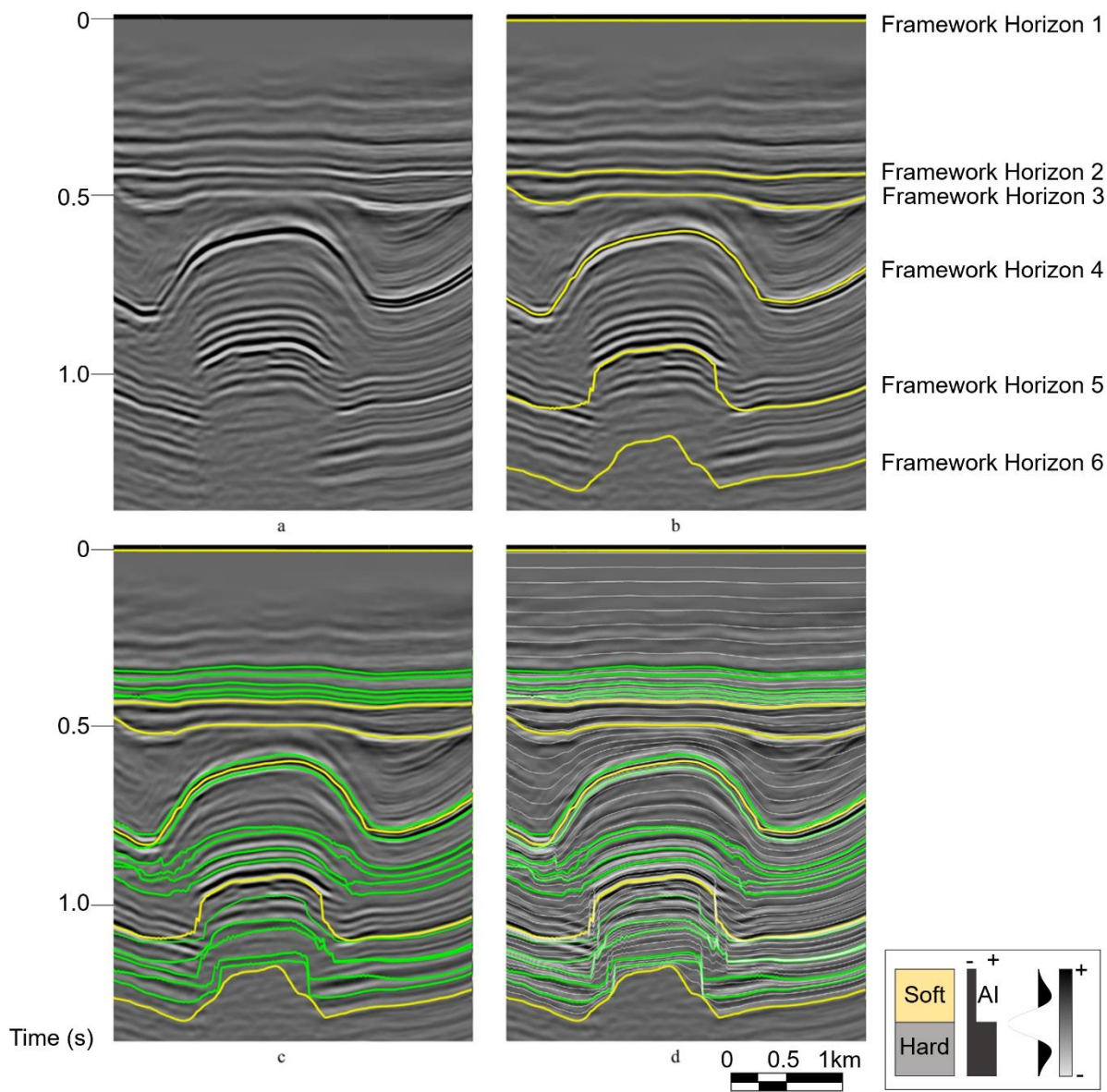


Figure 5. Stepwise creation of a dense set of horizons: a) Inline 2588, b) Framework horizons (yellow), c) User-guided infill horizons (green), d) Model-driven infill horizons (white, every fourth horizon is shown).